World Academy of Science, Engineering and Technology
International Journal of Computer and Information Engineering
Vol:6, No:12, 2012

Adaptive Digital Watermarking Integrating Fuzzy Inference HVS Perceptual Model

Sherin M. Youssef, Ahmed Abouelfarag, and Noha M. Ghatwary

***Abstract*—**An adaptive Fuzzy Inference Perceptual model has been proposed for watermarking of digital images. The model depends on the human visual characteristics of image sub-regions in the frequency multi-resolution wavelet domain. In the proposed model, a multi-variable fuzzy based architecture has been designed to produce a perceptual membership degree for both candidate embedding sub-regions and strength watermark embedding factor. Different sizes of benchmark images with different sizes of watermarks have been applied on the model. Several experimental attacks have been applied such as JPEG compression, noises and rotation, to ensure the robustness of the scheme. In addition, the model has been compared with different watermarking schemes. The proposed model showed its robustness to attacks and at the same time achieved a high level of imperceptibility.

***Keywords*—**Watermarking**,** The human visual system (HVS), Fuzzy Inference System (FIS), Local Binary Pattern (LBP), Discrete Wavelet Transform (DWT).

I. Introduction

DUE to the increase of the digital media usage and sharing it through the internet a persuasive limitation is needed to handle the duplication of the data. The media security became one of the most important issues to ensure copyright protection and illegal distribution. Watermarking is one of the capable solutions to insure the ownership verification of a digital media by embedding an invisible signal into the multimedia data [1]. The watermark can be classified in to two types, either visible watermark or invisible watermark. Robustness against signal processing or different types of attacks is one of the main properties of watermarking. These attacks can include jpeg compression, noises, median filter, rotation, etc. Different types of watermarking application and types of attacks are explained in [2-4], [9].

There are two important contradicting requirements for embedding a watermark in an image that a robust watermark should be embedded into the most perceptually significant regions of the host image. However, to be undetectable to the human visual system (HVS), a robust watermark should be placed in the most perceptually insignificant regions of the host image.

The watermarks can be applied in of the two domains either in spatial domain or frequency domain. The computational overhead results for the spatial domain compared with frequency domain are less [13]. The spatial domain watermark techniques are developed early [12], the embedding watermark process is simple but the signals are easily noticed, corrupted or removed. The frequency domain approach has more advantages as the signal processing operations can be well categorized [1].

The Human visual system (HVS) has been considered with several phenomenon that permits to adjust the pixel values to elude perception. The spatial masking distinguishing of the human visual system describes the Ability of the HVS to sense pixel elements that are altered in homogenous regions with more ease than in regions with large contrast [11]. The presented model implements an adaptive watermarking scheme that integrates a fuzzy inference system with the characteristics of the human visual system. The strength of the watermarking is regulated based on the combination of the HVS and Fuzzy Inference System (FIS) to embed on the wavelet transform of an image.

This paper is organized as follows. Section II represents the related work of different watermarking schemes, the problem formulation is illustrated in section III while the Experimental results are illustrated in section IV and the conclusions are discussed in section V.

II. Related Work

A current trend towards methodologies that make use of information about the human visual systems (HVS) to watermark signal has been in continues increase [6]. Approaches has been made by using wavelet domain for watermarking that proposed the highest information hiding capacity for embedded signal.

Discreet Wavelet Transform (DWT) is know that the wavelet image/video coding and play an important role in image/video compression standards, such as JPEG and MPEG due to its excellent performance in compression. Sathik et al [3], proposed a DWT based invisible watermarking technique by using Arnold and Fibonacci Transform. A fuzzy watermarking system that embeds in the wavelet sub-bands was adopted by Oueslati *et al* [4] to protect medical images by embedding in the middle sub-band frequencies. Sakr *et al*[17] , introduces a watermarking scheme based on dynamic fuzzy inference system, that generates a dynamic system for the feature evaluation to embed in the image based on human

S. M. Youssef is with Department of Computer Engineering, College of Engineering and Technology, AAST, Alexandria, Egypt(phone:203-5622366,email:sherin@aast.edu).

A. A. Elfarag is with Department of Computer Engineering, College of Engineering and Technology, AAST, Alexandria, Egypt(phone:203-5622366,email:Abouelfarag@aast.edu).

N. M. Ghatwary is with Department of Computer Engineering, College of Engineering and Technology, AAST, Alexandria, Egypt(phone:203-5622366,email:nohaghatwary@gmail.com).

visual system quantative values.

In [7], Barni *et al* put forward an evaluation method of optimum weighting factor based on visual concerns in the DWT coefficients. Barni *et al* focused their work on highly textured area as the eye is less sensitive of these regions. Lin Q. et al [22], proposed a scheme of DWT embedding by implementing a DSP to insure the invisibility to HVS. In [16], Toa *et al* adopt a discrete wavelet transform based on multiple watermarking algorithms. To ensure robustness the watermark was embedded in the high frequency sub-bands of DWT.

III. The Proposed Model Description

The presented model integrates the multi-resolution wavelet analysis with the proposed fuzzy inference based architecture to produce the perceptual gain represented as a weight gain factor (α). The gain factor will be used to control the selection criteria to allocate candidate location for watermark embedding.

Fuzzy logic is used for data fusion and operates on the HVS model for spatial masking in a wavelet domain. A fuzzy-based block selection scheme has been proposed based on the media visual characteristic variables (brightness, texture and gradient) computed for each block wavelet coefficients in the image. The output of the fuzzy system is a single value which gives a perceptual value for each corresponding block coefficients. The FIS is designed to generate the weight gain factor of the selected pixel in each of in the candidate blocks based on the HVS criteria for Brightness, Texture and Edges of the image.

Each image is first divided into a set of non-overlapping blocks, each of the size N*N. As shown in Fig.1. The selected blocks are exposed to 2D Discreet Wavelet Transform (DWT). The advantage of using the DWT over other transforms that it consummate the HVS. This property is one of the main benefits that support the embedding process of watermark in the areas where the HVS is less sensitive to it [14] ,[10].

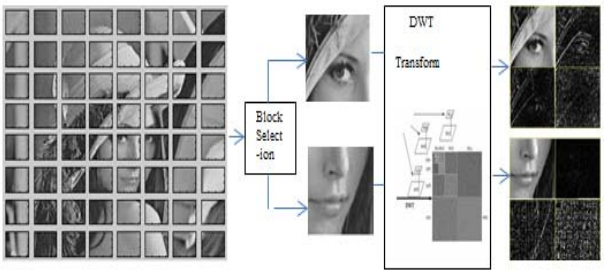

Fig. 1 The image block division and Block DWT

Different phases have been introduced including image sub-block division, multi-resolution analysis of each sub-region division using wavelet transform, extraction of HVS properties of the each block, the proposed Fuzzy Inference System architecture (FIS), fuzzy-based sub-region selection, watermark generation and encryption using pseudo random key generator, generating stego watermarked image using inverse wavelet transform.Fig.2 illustrates a block diagram of the proposed model which demonstrates the scheme of the watermarking process. In the following sub-sections, each phase will be described in details.

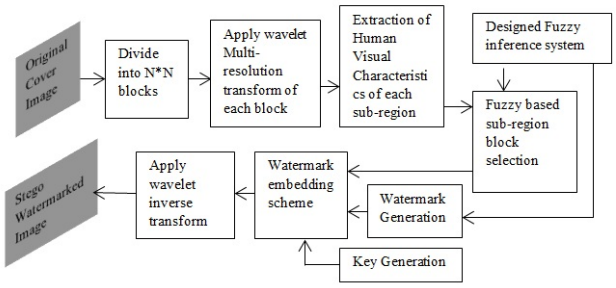

Fig. 2 The proposed model architecture

A. Fuzzy Inference System

The FIS has been implemented to adapt the HVS different properties. In the proposed scheme we are considering texture, brightness and edge sensitivity. This approach is designed in such a manner to enable the visual sensitivity membership function to fit the properties of an image.

In this section, each HVS property used is described. The visual formulations are discussed with an illustration on the membership function creation to adapt to the properties of the image. The output of the FIS is gain factor for the built membership functions is described in the defuzzification section with an overview of the rule base system.

1. Texture sensitivity (T)

The stronger the texture the lower the visibility of the embedded signal, so therefore we search for the pixels with the highest texture to embed the watermark in it.

In the proposed approach, the texture sensitivity is calculated based on Local Binary Pattern (LBP). The LBP is an operator that was first introduced by Ojala et al. [19] based on the postulation that texture has locally two paired aspects, a pattern and its strength. The effectiveness has been proposed to be an operative descriptor in texture classification [20].

Recently, the LBP became one of the strongest measures of texture analysis in an image, which show high results in a lot of experimental studies [21]. The LBP operator can be comprehended as a uniting methodology to the traditionally different statistical and physical models of texture analysis. In [21], it was stated that "the most important property of the LBP operator in real-world applications is its invariance against monotonic gray level changes".

The LBP is defined as a gray-scale invariant texture measure, resulting from a description of texture in a local neighborhood. A binary value from 0 to 255 is gained by concatenating the values of the neighborhood results in a clock wise direction for each pixel. As shown in Fig. 3 below, the membership function of the texture is classified in to four membership functions to fit the image's texture properties based on the variance distributed among smooth, slightly smooth, slightly rough and rough.

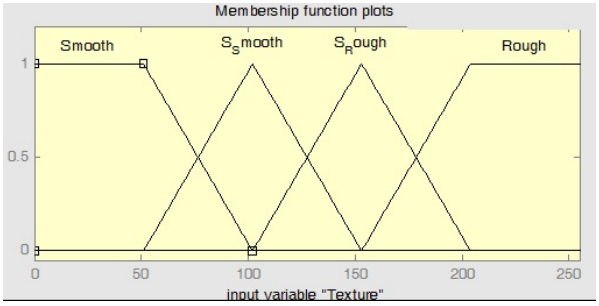

Fig. 3 Texture Fuzzy Membership Function

2. Brightness Sensitivity (*B*)

The visibility of brighter background are less sensitive than dark ones , That way our model search for pixel with high brightness values to embed the watermark bit in it.

As for gray scale image, the value of the pixel represented can be used as the brightness value of the pixel. The most common pixel format is the byte image that results in a value from 0 to 255 as the numbers are stored in an 8-bit integer form. The pixel value '0' represents the maximum darkness while the '255' represents the maximum brightness. The grey shades are represented in the values in between.

The Brightness sensitivity membership function is enabled to be adjusted in such a manner to best fit the image's properties as shown in Fig.4. Each input is composed of three membership function based on the variance distributed among Dark, Dim and Bright.

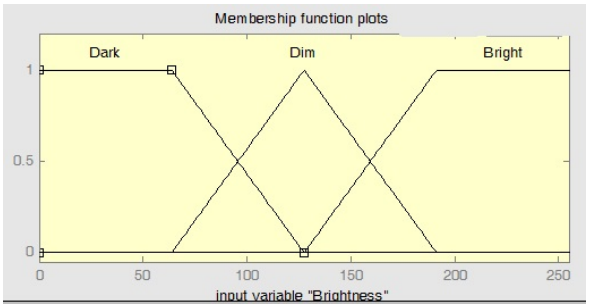

Fig. 4 Brightness Fuzzy Membership Function

3. Edge Sensitivity (*E*)

The higher the edge the lower the visibility of embed signal, so therefore the embedded watermark is inserted in the higher edges. A gradient analysis has been made to test the model by using different edge detection methods such as canny, sobel and prewitt. Fig. 5 shows the Edge sensitivity membership function that is composed of two membership function between high and low as the results of the canny edge detector result in two output either '0' where edges are not found and '1' for edged surface.

B. Defuzzification

The defuzzified output f is calculated for the composite output set. The fuzzy results generated cannot be used as such to the applications, hence it is necessary to convert the fuzzy quantities into crisp quantities for further processing. We used the centroid defuzzification method that returns the center of area under the curve by using (1). Where the inferred value f represents the weight gain factor from fuzzy inference system of a specific input, μ_n is the aggregated subsequent membership function of the output fuzzy sets and f_b is the universe of discourse corresponding to the centroid of μ_n.

$$f = (\int \mu_n(f_b) f_b \, df) / \int \mu_n(f_b) df \quad (1)$$

The output of the FIS is gain factor for the particular block is divided into five membership function very small, small, average, almost large, and large as shown in Fig. 6. This block calculates the mean and the variance of the image block. The calculated variance is feed to the FIS. The fuzzy rules and the membership function were developed using intuitive logic and the characteristics of human visual system.

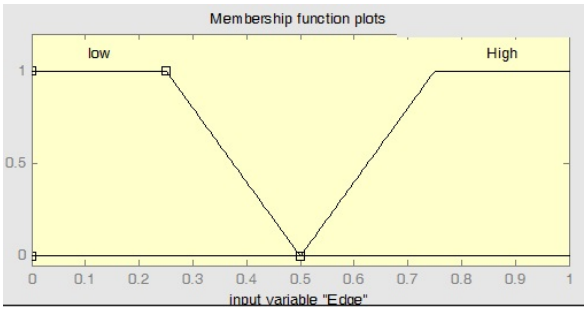

Fig. 5 Edge Fuzzy Membership Function

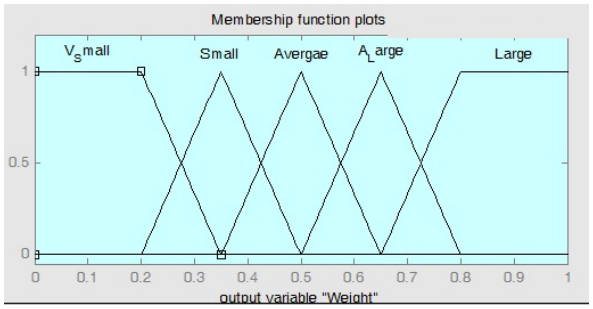

Fig. 6 The output membership function

A small view of the simple fuzzy rules is illustrated as follow:

1. If <Brightness> is Dark and <Texture> is smooth and <Edge> is low then <Weight> is very small.
2. If <Brightness> is Dark and <Texture> is slightly smooth and <Edge> is low then <Weight> is very small.
3. If <Brightness> is Dark and <Texture> is smooth and <Edge> is high then <Weight> is small.
4. If <Brightness> is Dark and <Texture> is slightly smooth and <Edge> is high then <Weight> is Average.
5. If <Brightness> is Dark and <Texture> is rough and <Edge> is high then <Weight> is Almost Large.
6. If <Brightness> is Dim and <Texture> is smooth and <Edge> is low then <Weight> is very small.
7. If <Brightness> is Dim and <Texture> is slightly rough and <Edge> is low then <Weight> is small.

8. If <Brightness> is Dim and <Texture> is slightly rough and <Edge> is high then <Weight> is Average.
9. If <Brightness> is Dim and <Texture> is rough and <Edge> is high then <Weight> is very Almost Large.
10. If <Brightness> is Bright and <Texture> is smooth and <Edge> is low then <Weight> is very small.
11. If <Brightness> is Bright and <Texture> is slightly smooth and <Edge> is low then <Weight> is small.
12. If <Brightness> is Bright and <Texture> is slightly rough and <Edge> is low then <Weight> is Average.
13. If <Brightness> is Bright and <Texture> is slightly rough and <Edge> is high then <Weight> is Almost Large
14. If <Brightness> is Bright and <Texture> is rough and <Edge> is high then <Weight> is Large.

These rules calculate the amount of gain for the particular pixel. In Fig. 7 a snap-shot of rule viewer is shown on how the output is affected by values of the input. Also, a surface view between texture and edge is shown in Fig. 8.

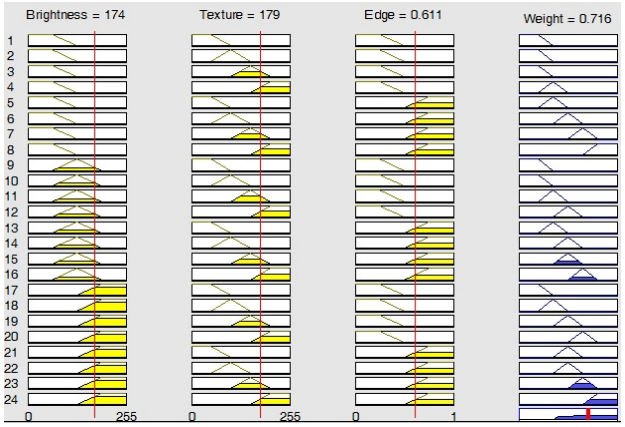

Fig. 7 Snapshot of Rule Base Viewer

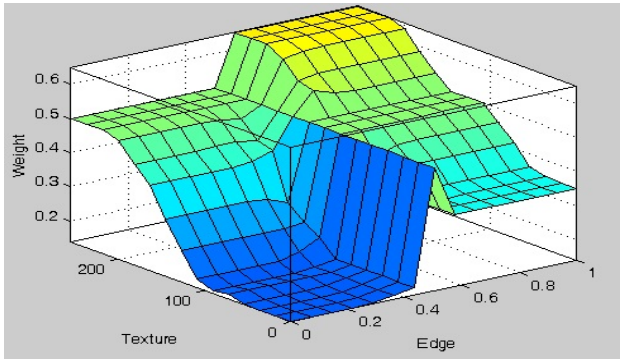

Fig. 8 Surface area view of texture and edge

C. Multi-resolution analysis Using Discrete Wavelet Transform

1. Discrete Wavelet Transform (Overview)

Wavelet analysis has been widely used in the image processing because of the unique characteristics and advantages of signal analysis, especially in the field of image retrieval. The dominant time-frequency analysis enables the image properties to be described and provides a feasible way for high-accuracy retrieval system. More information about DWT can be found at [23].

The Wavelet Transform (WT) is a technique for analyzing signals. It was developed as an alternative to the short time Fourier Transform (STFT) to overcome problems related to its frequency and time resolution properties. More specifically, unlike the STFT that provides uniform time resolution for all frequencies the DWT provides high time resolution and low frequency resolution for high frequencies and high frequency resolution and low time resolution for low frequencies. The Discrete Wavelet Transform (DWT) is a special case of the WT that provides a compact representation of a signal in time and frequency that can be computed efficiently. The DWT is defined by (2)

$$W(j,k) = \sum_j \sum_k \left[x(k) * 2^{-j} * \psi(2^{-j} * n - k) \right] \qquad (2)$$

where ψ(t) is a time function with finite energy and fast decay called the mother wavelet.

2. Applying DWT for block sub-regions

DWT is used to analyze the image into different frequency components at different resolution scales (i.e. multi-resolution). Allows revealing image's spatial and frequency attributes simultaneously. The 2D-DWT decomposes the image into four subbands into four sub-bands LL, LH, HL, HH. The sub-bands, corresponding to approximate, horizontal, vertical, and diagonal features, respectively. The LL subband is approximately located at half the original image. While, the HH subband contains the high frequency details if image. On the other hand, the HL-LH convey changes of image[25].

The presented model merges between the benefits of the DWT transform to formulate the weight gain factor (α) from FIS. As most of the energy of the image is located in the LL sub-band, we use it to calculate the gain factor (α), while the embedding process happens in the HH sub-band region it holds most of the texture and edges of the images where usually the human eye is not sensitive to these areas. This insures the invisibility for the eye.

D. Block Selection Criteria

A fuzzy-based Block Selection Scheme (FBSS scheme) has been proposed to select candidate sub-blocks for watermark embedding. The visual characteristics of each block have been extracted, including texture, brightness and edges. These characteristics have been exposed to a Fuzzy Inference system; which has been designed, to produce a Block Participation Strength Factor (δ). Correspondingly, only sub-regions of the image are selected for embedding using the proposed fuzzy visual model.

An averaging technique is used to calculate the HVS for each block. Accordingly, the brightness, texture and edge are extracted from each the block and a mean value are calculated for each block. This generates a strength sensitivity factor of block to decide wither it a candidate or not compared to the remaining blocks.

E. Watermark Generation

Watermark generation unit generates the necessary watermarking bit. This block has two inputs: the Fuzzy weight factor and the watermarking bit. The watermark binary image is divided into 8*8 blocks where each watermark block results in 64 bit used to watermark one of the image block candidates.

As shown in Fig. 9, The selected blocks are applied to the FIS to generate the weight gain factor (α) for all the pixels in the block then a selection criteria is applied to choose the highest 64 weight factors to start the embedding process in it.

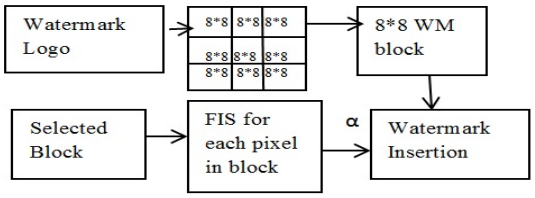

Fig. 9 Watermark Generation process

F. Watermark Embedding Process

The watermark is embedded in the DWT HH sub-band of the selected blocks. Each pixel in the HH sub-band is embedded according to (3)

$$I^*_{(x,y,k)} = I_{(x,y,k)} + [1 + W_{(x,y,k)} * \alpha] * \beta \quad (3)$$

where (x,y) represent the pixel reference , k represent the block number in the image. I* the watermarked image, I original image, α represents the gain factor gained from the designed FIS the β represents the key.

G. Watermark Extraction Process

The extraction process is kind of similar to the embedding process as the image is again divided in N*N blocks, a key is sent to the receiver to detect the candidate blocks so the watermark can be detected. The extraction is non-blind as the receiver has the original image. The candidate block is exposed to the FIS and the weight factor is regenerated to embedded image referring to (4).

$$W^*_{(x,y,k)} = ((I^*_{(x,y,k)} - I_{(x,y,k)}) / \beta) - 1) / \alpha \quad (4)$$

where the W* represents the extracted watermark.

IV. Experimental Results

The proposed model has been carried out on several experiments to test the efficiency of the model. The model has been tested using different benchmark images of different sizes. Also, different watermark logos of different sizes have been used in embedding and tested. Moreover, different results from our scheme have been compared with results of DWT image watermarking found in [3], [8], [18], [22], [24].

In this section we illustrate the performance indicators used to evaluate the proposed model on embedded and extracted watermarked images and watermark logos, before and after several types of attacks.

A. Performance Measure

In order to properly evaluate the performance of image watermarking schemes and to allow a fair comparison between different schemes, a benchmark suite must include a set of tests and a way of measuring the results of the tests using controlled conditions.

In watermarking, the tests are oriented to measure the requirements of an application. So, the *robustness*, the fidelity and the capacity are commonly measured:

1. Mean-Square-Error (MSE):

MSE is the cumulative squared error between the original and watermarked image as shown in (5).

$$MSE = 1 / \sum_{x=1}^{M} \sum_{y=1}^{N} [I_{(x,y)} - I'_{(x,y)}] \quad (5)$$

where M, N is the dimension of Image, I(x,y) is the original image, I' is the watermarked image.

2. Peak-Signal-To-Noise (PSNR)

PSNR expressed in (6) is one of the most common measures of distortion in the image field. PSNR is a useful tool to measure perceptibly level, it not always accurate to human eyes adjustment

$$PSNR = 10 \log_{10} (255^2 / MSE) \quad (6)$$

3. Normalized Correlation(NC):

NC measures the similarity between the original image and watermarked one, before and after extraction referring to (7). The value of NC is between 0 to 1. The bigger the value of the NC is the better the watermark robustness.

$$NC = (\sum_{x=1}^{M} \sum_{y=1}^{N} (I_{(x,y)} * I'_{(x,y)})) / (\sum_{x=1}^{M} \sum_{y=1}^{N} (I_{(x,y)})^2) \quad (7)$$

4. Bit Error Rate (BRE):

One of the most important performance measure indicators that defines the ratio of correctly extracted bits to the number of embedded bits as shown in (8).

$$BRE = EB / NB \quad (8)$$

where EB represents the number of incorrectly decoded bits and NB represents no. of total bits.

B. Proposed Model Results

Different experiments have been carried out to test and validate the proposed model using the different data sets. The performance indicators described above were used to provide statistical evaluation of performance. Example of the watermarking results is shown in Fig. 10.

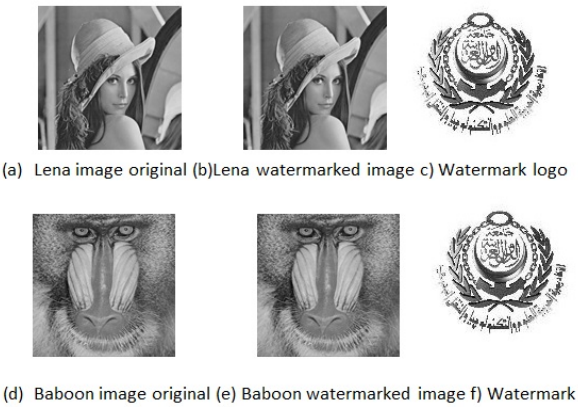

(a) Lena image original (b)Lena watermarked image c) Watermark logo

(d) Baboon image original (e) Baboon watermarked image f) Watermark logo

Fig. 10 Different images before and after watermark

In Table I the PSNR and BRE are calculated for different data set images with different watermark logos. The table results show an effective PSNR values and that the percentage of the bit rate error is very small that indicates the robustness and efficiency of the proposed model for different watermark logo sizes. Fig. 11 represents a snapshot from the watermark logos used of different sizes.

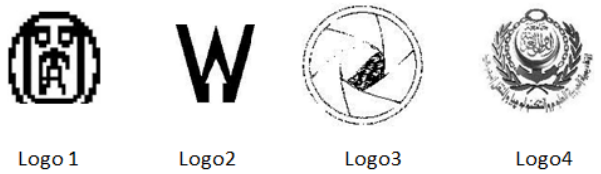

Fig. 11 Watermark logo with different sizes

TABLE I
PSNR AND BRE FOR DIFFERENT WATERMAKR LOGOS

PSNR & BRE	Pepper Image	Lena Image	Barbara	Baboon
PSNR Logo1(16*16)	77.6648	83.6854	75.726	76.612
BRE%	0.0266	0.0067	0.0439	0.0234
PSNR Logo2(32*32)	70.2473	72.416	68.309	71.200
BRE %	0.1548	0.0892	0.2382	0.1349
PSNR Logo3(40*40)	66.3954	71.6656	59.912	62.305
BRE %	0.3007	0.0929	0.3801	0.3127
PSNR Logo4(48*48)	59.6113	68.6656	56.367	57.610
BRE %	0.3102	0.1092	0.36	0.2122

Fig. 12 illustrates the change in the peak-signal-to-noise-ratio for different sizes of the embedded watermark, applied for different bench mark test images. As shown from the chart, the PSNR remains high for all test images. As the size of the watermark increase there is a slight decrease in the PSNR.

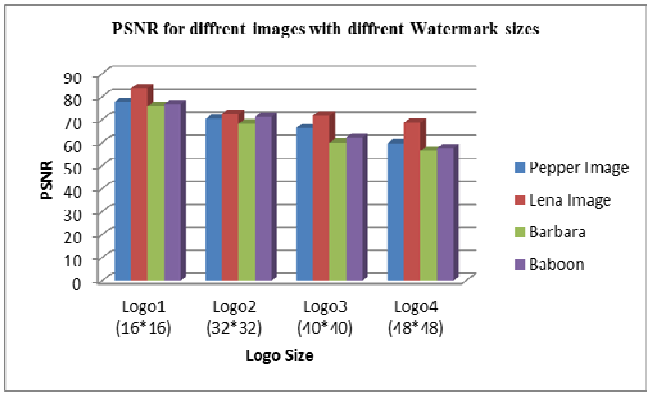

Fig. 12 PSNR Watermarked images with Diffrenet Watermark logo sizes

The dataset images have applied under different values of JPEG compression after embedding process. Fig.13 demonstrates the change of the PSNR for different percentages of JPEG compression results. As shown in the figure the PSNR remains high for the JPEG attacks ranging from 50 to 90, and small decrease occurs ranging from 20 to 40 JPEG compressions. This illustrates the robustness of the proposed model against JPEG compression.

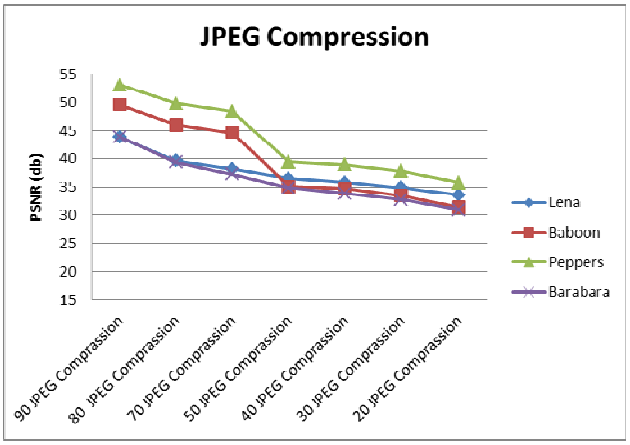

Fig. 13 PSNR for different images at different JPEG compression

Experiments also have been made on the extracted watermark logo after applying different values of salt and pepper noises. In Fig. 14, a view on the Barbara watermarked image and the extracted watermark after applying the noise at different percentages. To insure that the watermark logo survived the attack, the correlation between original watermark logo and the extracted one has been calculated after numerous experiments with different values of noise.

A demonstration of the correlation of extracted watermark after experiments on different images from data set with various percent is illustrated in Fig.15, The figure shows a high similarity between the embedded and extracted logo till high percentage of the noise. The chart shows as smooth decreases of correlation in parallel with the increase in the percentage of the salt and pepper noise increase.

Fig. 14 Stego image and Extracted watermark after different Salt and Pepper percentages images

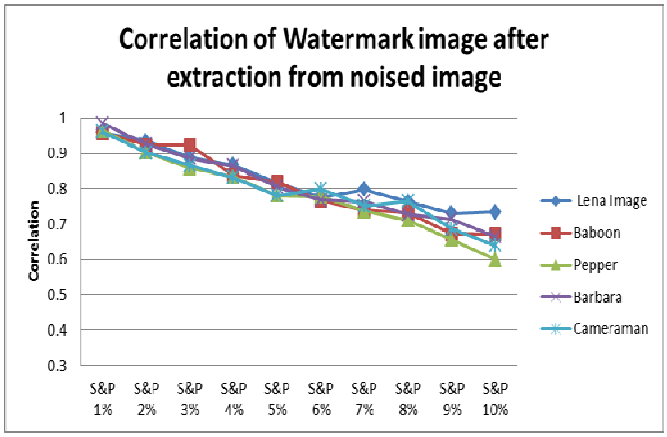

Fig. 15 Correlation of the Salt and Pepper noise attacks on extracted watermark from different image

In Tables II, III and IV, the performance of our proposed model was compared with Sathik et al, 2012 [3] and Sujatha et al, 2010 [8] for different types of attacks based on the cameraman image as shown in Fig. 16, of size 512*512 to insure the robustness.

(a) Cameraman image original (b) Cameraman watermarked image

Fig. 16 Camera man image of size 512*512 before and after embedding

Table II shows a comparison between the proposed model and different methods in the PSNR, MSE and NC in case of no attack on the cameraman image.

Table III and Table IV illustrates the results of different types of attacks on the proposed model based on the cameraman image of size (512*512). In order to evaluate the model, noises such as Gaussian and salt & pepper noises, median filtering, linear filtering, blurring, histogram equalization, JPEG compression and rotation were applied. The model was compared with results of methods presented in [8] and [3].

TABLE II
EVALUATION OF WATERMARKING SCHEME

Watermarked Image	Proposed Model	Sathik et al [8]	Sujatha et al [3]
PSNR(No attack)	68.3091	54.1047	59.1168
MSE (No attack)	0.0096	0.2527	0.0797
NC (No attack)	1	1	0.8496

The PSNR of the attacks are illustrated in Table III. The proposed model showed effectiveness against Gaussian noise, salt and pepper noise and histogram equalization. The model out performed against different JPEG compression, Median filtering attack and rotation at different degrees. There was a drop in the PSNR results in the linear filtering and blurring attack against other models.

TABLE III
PSNR VALUES OF SEVERAL TYPES OF ATTACKS

Attack Type	Proposed Model	Sathik et al [8]	Sujatha etal [3]
Gaussian (0.01,0)	41.5839	37.8092	38.3272
Gaussian (0.0.001)	33.0995	30.073	30.0997
Salt& pepper (0.002)	32.1454	32.0153	32.1381
Median Filter[3*3]	40.4849	29.5819	29.5727
Linear Filtering	7.4366	27.7792	27.7761
Blurring	31.4801	37.8281	37.8322
Histogram Equalization	19.0416	19.0192	19.0944
Rotation 5	19.0206	13.9478	13.9492
Rotation 10	19.0206	12.0324	12.0325
JPEG 90	53.2933	43.0143	43.1448
JPEG 70	53.2933	36.4452	37.4799
JPEG 50	41.3574	35.2058	35.4799
JPEG 30	39.1594	33.1859	33.2002
JPEG 10	33.1769	29.1818	29.1867

TABLE IV
NC VALUES OF SEVERAL TYPES OF ATTACKS

Attack Type	Proposed Model	Sathik et al [8]	Sujatha et al [3]
Gaussian Noise (0.01,0)	1	1	0.8371
Gaussian Noise (0.0.001)	0.9916	0.5229	0.5042
Salt and pepper (0.002)	0.9948	0.9880	0.837
Median Filter[3*3]	0.9992	0.5200	0.6629
Linear Filtering [3*3]	0.8488	0.5300	0.6696
Blurring	0.9915	0.6656	0.8083
Histogram Equalization	0.9392	0.7645	0.7498
Rotation 5	0.6977	0.5191	0.7135
Rotation 10	0.5406	0.4865	0.6957

Table IV presents the Normalized Correlation results applied on the Cameraman image (512*512) against different type of attacks. The results give an indication of the high validation of the watermarked image against the attacks. In Fig. 17, the comparison is continued between the models to compare the correlation after JPEG compression of the

watermarked image, the proposed model out performs the other techniques at different JPEG compression ratios.

The rotation attack was tested on the model as shown in Fig. 18 with Lin et al, 2009 [22] and Sujatha et al, 2012 [18], on the Lena image of size (512*512). As shown in the graph, at [22] there was a better performance at rotation at 10 degrees than proposed model. But as the rotation degree increased the PSNR of our presented model showed a comparable result to the other two methods.

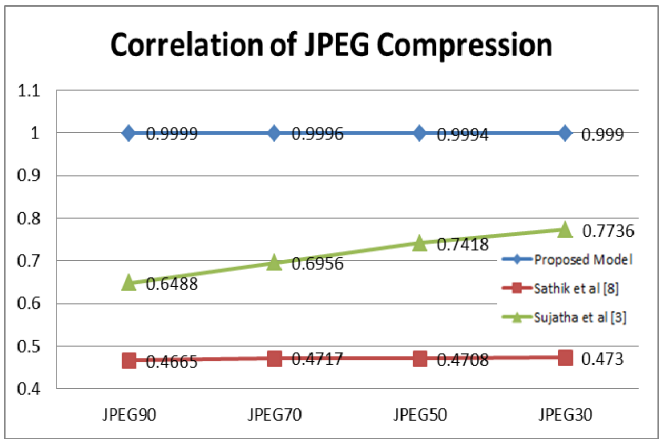

Fig. 17 Correlation of JPEG compression Between models

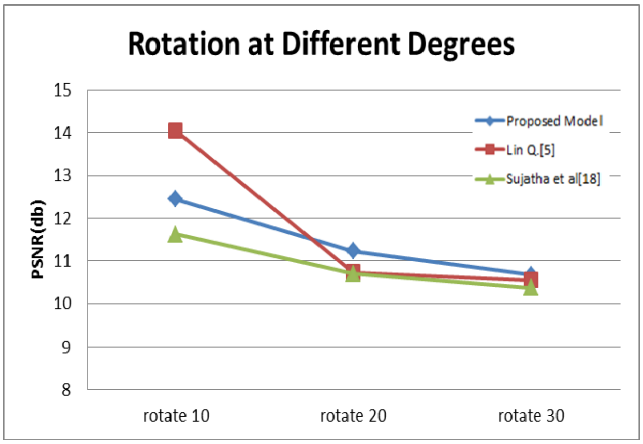

Fig. 18 PSNR for Rotation attack Between models

TableV shows another comparission made on the camerman image of size (512*512) with reults of Sujatha et al,2010[24]. The table includes different variances of the guassian noise, salt and pepper noise and median attack. The PSNR of the proposed model was analogous with the method in[24] in the case of gaussian as shown Fig. 19. For the salt and pepper attacks the values were compareble .While inmedian filter, the proposed model out showed a better performance in the proposed model. On the other hand, the perfomnce of NC flucate between 0.9990 to 1 against the several atacks.

TABLE V
PSNR AND NC FOR DIFFERENT YPES OF ATTACKS

Attacks		PSNR(dB)		NC	
		Proposed Model	Sujatha et al [24]	Proposed Model	Sujatha et al [24]
Adding Gaussian Noise (mean, variance)	[0.001,0]	68.3091	56.2083	1	0.9933
	[0.005,0]	49.0894	46.4663	1	0.9933
	[0.01,0]	41.5839	38.0920	1	0.9933
	[0.05,0]	29.8546	25.7482	1	0.9933
Salt and Pepper Noises	[0,0.001]	33.0995	30.0890	0.9917	0.5229
	[0,0.002]	32.1872	27.1712	0.9839	0.5145
	[0.001]	35.9226	35.1261	0.9978	0.9900
	[0.002]	32.1454	32.0256	0.9948	0.9859
	[0.005]	28.2855	28.0211	0.9875	0.9737
	[0.01]	25.1683	29.0211	0.9746	0.9595
Median Filter	[3*3]	40.4849	29.5542	0.9992	0.5789
	[5*5]	39.152	26.9883	0.9990	0.5981

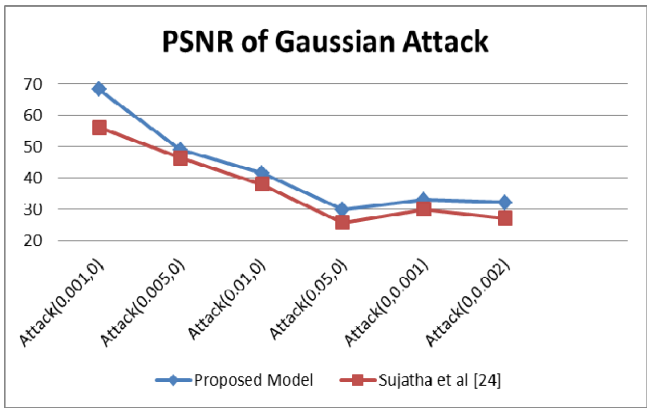

Fig. 19 PSNR of different values of Gaussian attack between models

V. CONCLUSION

This novel study, proposed an effective watermark technique the use Fuzzy wavelet coefficients of the proposed perceptual fuzzy inference system to embed watermark. The method is different from previous researches which use significant coefficients to embed a watermark.

The fusion between the HVS and FIS was used to adjust the weight gain factor that generates the watermark embed in an image without affecting its quality.

The model showed effective resist against several types of attacks especially JPEG compression and salt and pepper noises. This indicates the robustness of the model. Moreover, owing to the significant statistical difference, our method is more robust in cases of resistance against attacks by Gaussian noise with a variance of less than 2, as well as against filtering attacks which employ larger masks such as median filtering 3x3.

REFERENCES

[1] Hsieh.M., "Perceptual Copyright Protection Using Multi-Resolution Wavelet-Based Watermarking and Fuzzy Logic". International Journal of Artificial Intelligence & Applications (IJAIA), Vol.1, No.3, July 2010,pp 48-57.

[2] Manjula, R., & Settipalli, N. "A new Relational Watermarking Scheme Resilient to Additive Attacks". International Journal of Computer Applications, Vol. 10, No. 5, November 2010 pp 1-7.

[3] M.Mohamed Sathik and S.S.Sujatha,"A novel DWT based Invisible Watermarking Technique for Digital Images". *International Arab Journal of e-Technology,Vol. 2, No. 3,*. Pp167-173. January 2012.

[4] Oueslati, S., Cherif, A., & Solaiman, B., "A Fuzzy Watermarking System Using the Wavelet Technique for Medical Images", International Journal of Research and Reviews in Computing Engineering, Volume 1, No. March 2011,pp 3-8

[5] Podilchuk and C.I. Wenjun Zeng "Image-adaptive watermarking using visual models" Lucent Technol., Bell Labs., Murray Hill, NJ, IEEE Journal, vol.16, Issue: 4,pp. 525-539 ,May 1998. 5

[6] Cox, I. J., Miller, M. L., Bloom, J. A., & Way, I. "Watermarking applications and their properties", Int. Conf. on Information Technology2000.pp1-5.

[7] Barni M, Bartolini F, Piva A. "Improved wavelet-based watermarking through pixel-wise masking", IEEE Transactions on Image Processing 2001;10:783-91.

[8] Sujatha S.S, Sathik M.M,"A novel Pixel Based Blind Watermarking Algorithm by Applying Fibonacci Transform", Proc of ACM, September 20120, pp 197-202.

[9] S.P. Mohanty , K.R. Ramkrishnan and M.S. Kankanhalli, "An Adaptive DCT Domain Visible Watermarking Technique for Protection of Publicly Available Images" in International Conference on Multimedia Processing and Systems, Chennai, India, August 13-15, 2000.

[10] Der-Chyuan Lou, Te-Lung Yin, and Ming-Chang Chang," Robust Digital Watermarking Using Fuzzy Inference Technique", Journal of C.C.I.T., Vol.32, no.2, may 2004.

[11] Lande, P. U. "A Fuzzy Logic Approach To Encrypted Watermarking For Still Images In Wavelet" ,2010, pp 1-10.

[12] Schyndel, R. G., Tirkel, a. Z., & Osborne, C. F. (n.d.)., " A digital watermark", Proceedings of 1st International Conference on Image Processing, IEEE Vol 2, ,pp 86-90.

[13] Available Online at www.jgrcs.info Improving Security And Reducing Effect Of Attacks On. (2011)., 2(7), 111-113.

[14] Jabade, V., Gengaje S., "Literature Review of Wavelet Based Digital Image Watermarking Techniques", International Journal of Computer Applications ,Volume 31– No.1, October 2011, pp 28-35.

[15] Huang, D., Member, S., Shan, C., Ardabilian, M., Wang, Y., & Chen, L. "Local Binary Patterns and Its Application to Facial Image Analysis" : November 2011, Vol.41, No.6, pp 765-781.

[16] Tao P., Eskicioglu A>M,"A robust multiple watermarking scheme in the discrete wavelet transform domain", Proceedings of the SPIE, Vol. 5601, 2004, pp 133-144.

[17] Sakr, N.; Jiying Zhao; Groza, V.; "Adaptive image watermarking based on a dynamic fuzzy inference system," Electrical and Computer Engineering, 2005. Canadian Conference on 1-4 May 2005, pp.976-979.

[18] S.S.Sujatha and M.Mohamed Sathik "A Novel DWT Based Blind Watermarking for Image Authentication".*International Journal of Network Security,,Vol. 14, No. 4,*. P223-228. July 2012.

[19] T. Ojala, M. Pietikäinen, and T. Mäenpää, "Multiresolution gray-scale and rotation invariant texture classification with local binary patterns", IEEE Trans. PAMI, vol. 24, 2002, pp. 971- 987.

[20] R.M. Haralik, K. Shanmugam, and I. Dinstein, "Texture features for image classification", IEEE Trans. SMC, vol. 3,, 1973,pp. 610-621.

[21] Pietikäinen, M. "Image Analysis with Local Binary Patterns", 2005, pp 115-118.

[22] Lin Q.,Liu Z.,Feng G.,"DWT based on watermarking algorithm and its implementing with DSP, IEE Xplore, 2008, pp229-232.

[23] Weeks, M., "Precision for 2-D discrete wavelet transforms processors". 2000 IEEE Workshop on Signal Processing Systems. SiPS 2000. Design and Implementation (Cat. No.00TH8528), pp 80-89.

[24] Sujatha, S.S.; Sathik, M.M.; "Feature based blind approach for robust watermarking," Communication Control and Computing Technologies (ICCCCT), 2010 IEEE International Conference , on 7-9 Oct. 2010, pp.608-611.

[25] Kinage,K.S and Bhirud,S.G;"Face Recognition based one Two-Dimensional PCA on Wavelet Subban", International Journal of Recent Trends in Engineering, Vol 2, No. 2, November 2009.